# CrystEngComm

## RSC Publishing

## COMMUNICATION

# Formaldehyde-assisted synthesis of ultrathin Rh nanosheets for applications in CO oxidation†

Changping Hou,[a] Jing Zhu,[b] Chang Liu,[a] Xue Wang,[a] Qin Kuang*[a] and Lansun Zheng[a]

**Ultrathin Rh nanosheets with a thickness of approximately 1 nm were synthesized *via* a simple surfactant-free hydrothermal route, using Rh(II) acetylacetonate as the precursor and formaldehyde as the shape controller. CO and H₂ originating from the formaldehyde decomposition played key roles in the formation of ultrathin Rh nanosheets.**

Shape controlled syntheses of noble metal nanoparticles have attracted intensive attention because of their shape-dependent properties in many application fields, such as catalysis, sensing, *etc.*[1] In diverse shapes of noble metal nanoparticles, two-dimensional (2D) ultrathin nanostructures have received particular interest, considering their large surface area and possible quantum size effects due to the exceptionally small thickness.[2] The present synthetic strategies essentially take effect through thermodynamic control and/or kinetic control over the growth of nanocrystals.[1b] For thermodynamic control, organic surfactants, which act as capping reagents to tune the growth behavior of nanocrystals by selective adsorption on the specific facets, usually play vital roles in the shape control of metal nanoparticles. However, surfactants can lead to some adverse effects in applications of noble metal nanoparticles due to their 'unclean' surface. Recently, it has been demonstrated that small adsorbates (*e.g.*, I⁻, CO) potentially act as good shape controllers for noble metal nanoparticles thanks to their particular advantages, such as high specificity and convenient removal from the surface of nanocrystals, and the as-synthesized noble metal nanoparticles exhibit excellent catalytic performances.[1b,2a,3] In view of this, it is highly desirable to explore similar surfactant-free synthetic routes for acquiring more specific shaped noble metal nanoparticles.

Rhodium (Rh) nanoparticles are known to exhibit extraordinary catalytic properties in diverse organic transformations as well as CO oxidation.[4] Considering the indispensability in catalysis and the preciousness of Rh, great effort has been devoted to the precise control of size and morphology of Rh nanoparticles, aimed at improving their selectivity and catalytic activity.[5–8] To date, various shapes of Rh nanoparticles, including nanocubes,[5] multi-pods,[6] tetrahedra,[7] and nanoplates,[8] have been synthesized. To our knowledge, however, most of the aforementioned cases were achieved in the organic phase (*e.g.*, oleylamine) or with the assistance of polymeric surfactants (*e.g.*, PVP). Herein we reported a simple formaldehyde-assisted solvothermal route to synthesize ultrathin Rh nanosheets (NSs) with a thickness of approximately 1 nm. Our experiments revealed that formaldehyde, which can decompose into H₂ and CO under solvothermal conditions, played dual roles as both the reducing and shape-controlling actions in the formation of ultrathin Rh NSs. Such ultrathin Rh NSs exhibited good catalytic activity in CO oxidation, thanks to their surfactant-free surface.

In a typical synthetic procedure of ultrathin Rh NSs, 20 mg Rh(II) acetylacetonate (Rh(acac)₃) and 0.8 mL of formaldehyde were dissolved in *N,N*-dimethylformamide (DMF, 9.2 mL), followed by a solvothermal treatment at 160 °C for 24 h (see synthetic details, ESI†). The morphology of the product was characterized by transmission electron microscopy (TEM). Note that the dispersion medium used in TEM sample preparation is crucial for the morphology observation of ultrathin Rh NSs. In Fig. 1a, it can be seen that the two-dimensional bamboo raft-like assemblies were formed, when dispersed in the common solvent ethanol. This is because Rh nanosheets dispersed in ethanol are apt to be self-assembled with each other in the face-to-face mode in order to reduce the total surface energy. The electron diffraction (ED) pattern displays a series of diffraction rings, which are well indexed to the (111), (200), (220), and (311) planes of the fcc-structured Rh from inside outward. The corresponding high-magnification TEM image (Fig. 1b) reveals the thickness of Rh NSs is very uniform. Based on the analysis of more than 100 Rh NSs from different stacks, the thickness of ultrathin Rh NSs is in the range of 1.0 ± 0.3 nm, with an average thickness of approximately

*[a] State Key Laboratory for Physical Chemistry of Solid Surfaces & Department of Chemistry, College of Chemistry and Chemical Engineering, Xiamen University, Xiamen 361005, China. E-mail: qkuang@xmu.edu.cn; Fax: +86-592-2183047; Tel: +86-592-21837879*
*[b] Department of Chemical and Biochemical Engineering, College of Chemistry and Chemical Engineering, Xiamen University, Xiamen 361005, China*
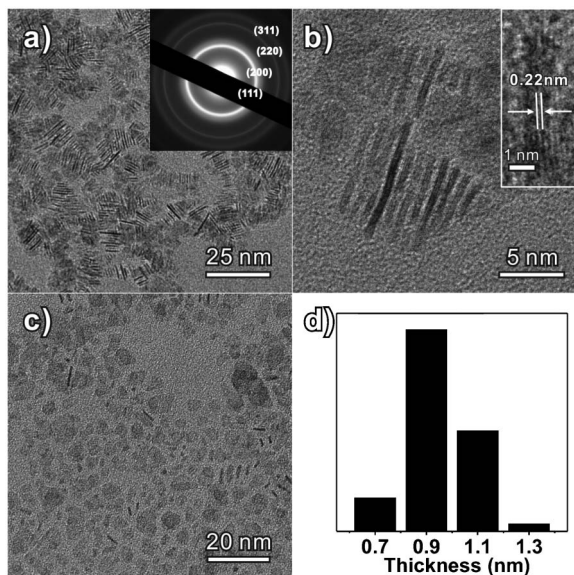
**Fig. 1** (a) Low-magnification and (b) high-magnification TEM images of the assembled ultrathin Rh NSs dispersed in ethanol; insets are the corresponding ED pattern and HRTEM image of an individual vertical Rh nanosheet. (c) TEM image of the lying Rh NSs dispersed in hexane. (d) The thickness distribution of ultrathin Rh NSs counted from the assembled ultrathin Rh NSs.

1 nm (Fig. 1d). High resolution TEM (HRTEM, the inset of Fig. 1b) further reveals that the layer spacing of the ultrathin Rh NSs is around 0.22 nm, corresponding to that of the (111) planes in the face-centered cubic (fcc) structured Rh. To observe the real and unassembled morphology of Rh NSs, the dispersion medium was specially changed to *n*-hexane (see the experimental details in ESI†). As shown in Fig. 1c, most of the Rh NSs are lying flat on the Cu grid, and the size is in a wide range of 5–20 nm, with the mean value around 10.6 nm. Note that the slight widening of the diffraction rings and the slightly obscure HRTEM image suggest that the crystallinity of such ultrathin Rh nanosheets is not so good. No diffraction peaks of Rh were actually recorded in the powder X-ray diffraction (XRD) pattern of the as-prepared product. A similar phenomenon was also found previously concerning other ultrathin nanoplates.[8] The disappearance of the XRD peaks might be attributed to the fact that the crystallographic periodicities in the ultrathin Rh NSs is too few. More valuable information about the composition of ultrathin NSs was provided by X-ray photoelectron spectroscopy (XPS) analysis. In Fig. 2, it can be seen that the Rh 3d signals of the product can be resolved into three components. The overwhelming peaks (the blue curve) at 307.2 eV and 311.9 eV are attributed to $3d_{5/2}$ and $3d_{3/2}$ of Rh(0), respectively, while their shoulder peaks located at higher binding energies should arise from other species of ionic Rh. Therein, the peaks at 308.3 eV and 313.0 eV correspond to partially reduced Rh components (*i.e.*, $Rh^{x+}$) and the peaks at 309.9 eV and 314.6 eV are due to the precursor $Rh(acac)_3$. The above XPS analysis demonstrates that the metallic Rh is the predominant species in the product.

To explore the formation mechanism of ultrathin Rh NSs, experiments with different amounts of formaldehyde were carried
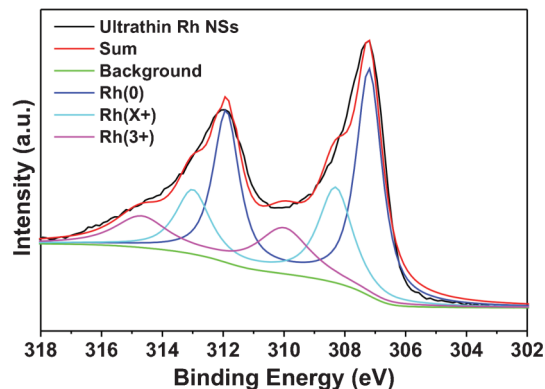


**Fig. 2** Rh 3d XPS signals recorded from as-prepared Rh NSs deposited on a silicon wafer.

out. In the absence of formaldehyde, the color of the reaction solution turned from yellow to a little darker, which is distinct from the color change of the ultrathin Rh NSs (Fig. S1, ESI†), and the resulting product was composed of nanoparticles of 1–3 nm in size (Fig. 3a). The formation of Rh nanoparticles indicates that the solvent DMF is poorly able to reduce a part of the precursor $Rh(acac)_3$ with most of the precursor remaining in the reaction solution. With the addition of formaldehyde (0.2 mL), the ultrathin Rh NSs were generated (Fig. 3b). The co-presence of some amorphous particles in the product indicates that the precursors are not completely reduced to metallic Rh due to insufficiency of formaldehyde. When the amount of formaldehyde was increased to 0.8 mL, most of the amorphous particles finally disappeared (Fig. 1a). However, the addition of too much formaldehyde (1.6 mL) would cause the formation of a large amount of Rh nanoparticles because of the too fast nucleation rate (Fig. S2, ESI†).

From the above results, it can be concluded that formaldehyde plays a crucial role in the formation of ultrathin Rh NSs. It is well known that formaldehyde would dissociate to carbon monoxide and hydrogen on metal catalysts ($HCHO \rightarrow H_2 + CO$).[3a,9] To distinguish each effect of CO and $H_2$, a series of proven experiments without formaldehyde were carried out in different atmospheres. Firstly, a CO gas flow was introduced in a sealed bottle keeping the system pressure at 0.2 MPa. After reaction at
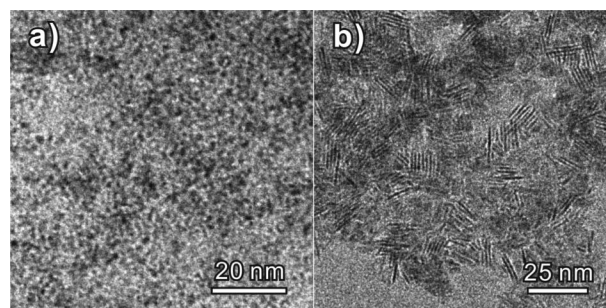


**Fig. 3** TEM images of Rh nanoparticles synthesized with different amounts of formaldehyde: (a) 0 mL; (b) 0.2 mL.
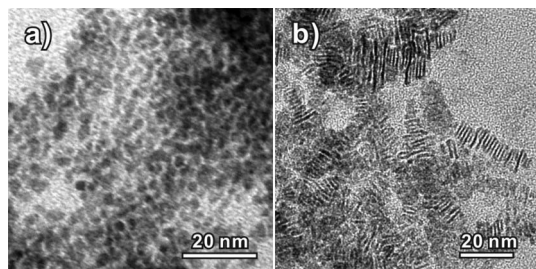
**Fig. 4** TEM images of Rh nanoparticles synthesized under different atmospheres: (a) $H_2$, (b) CO and $H_2$ mixed gas.



**Fig. 5** CO conversion over Rh nanocatalysts loaded on $CeO_2$ (black spot: Rh NSs synthesized by formaldehyde as reductant; red spot: Rh particles synthesized by acetaldehyde as reductant; green spot: the $CeO_2$ support).

160 °C for 24 h, the color of the reaction solution remained yellow, and no product was collected. By contrast, Rh nanoparticles of 3–5 nm were formed in a $H_2$ gas flow (Fig. 4a), while ultrathin Rh NSs were achieved in the coexistence of CO and $H_2$ (Fig. 4b). The above results reveal that $H_2$ is primarily liable for the reduction of the precursor $Rh(acac)_3$ to metal Rh(0), and CO is largely responsible for the surface control of products. Previous studies have demonstrated that CO prefers to specifically chemiadsorb on the {111} faces of fcc-structured Pd, thereby producing NSs via 2D anisotropic growth under the strong confinement effect of CO.[2a] Convincing evidence for this mechanism was offered by Fourier transform IR spectra. The freshly prepared ultrathin Rh NSs displayed an obvious CO band at 2082 cm$^{-1}$, whereas no CO adsorption was observed on Rh nanoparticles (Fig. S3, ESI†).[3] To further verify the surface controller role of CO, a CO gas flow was introduced in the experiment with acetaldehyde displacing formaldehyde in the synthetic procedure, in which nanoparticles of 5–10 nm in size were originally obtained. With the assistance of CO, some Rh NSs were generated in the presence of acetaldehyde (Fig. S4, ESI†). All the above results clearly indicate that in the formation of ultrathin Rh NSs, $H_2$ mainly acts as the reducing agent and CO as the shape controller through specific adsorption.

It is noted that the size of ultrathin Rh NSs can be roughly tunable by adjusting the concentration of the precursor $Rh(acac)_3$. As the amount of the precursor was increased from 5 to 10, 20 mg, the mean size of the ultrathin Rh NSs increased from 4.4, to 7.2, and 10.6 nm (Fig. S5, ESI†). Interestingly, the thickness of ultrathin Rh NSs remains unchanged, around 1.0 nm, despite an obvious change in the size distribution. This is attributed to the strong surface confinement effect of CO on (111) faces of Rh.

It is well known that Rh is one of the most important catalysts for catalytic oxidation of CO.[10] Herein, the evaluation of catalytic activity of Rh NSs was performed in a fixed-bed reactor coupled online with a gas chromatograph, with Rh nanoparticles obtained by acetaldehyde as reference. To prevent the aggregation of Rh catalysts, Rh catalysts were loaded at 1 wt% on a $CeO_2$ support (Fig. S6, ESI†), which is a common support for Rh-based catalysts in a wide variety of reactions, including CO oxidation.[11] As shown in Fig. 5, the temperature for 100% conversion over two Rh-loaded $CeO_2$ catalysts are markedly reduced, compared to the blank $CeO_2$ support. Therein, ultrathin Rh NSs reach 100% conversion at 110 °C, and Rh nanoparticles at 120 °C. In addition, the starting conversion temperature of ultrathin Rh NSs (50 °C) is much lower
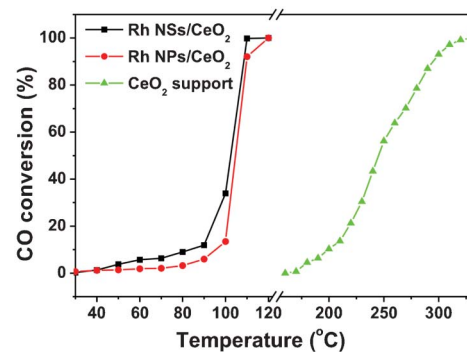
than that of Rh nanoparticles (90 °C). The enhancement in catalytic activity of $CeO_2$-supported Rh catalysts is attributed to the presence of Rh catalysts with a clean surface, which can lower the temperature of oxygen species (e.g., $O_2^-$) formation and facilitate the creation of oxygen vacancies.[11] The difference between catalytic activities of nanosheets and nanoparticles should be attributed to the shape effect from the ultrathin structure.[2]

In conclusion, ultrathin Rh NSs with a thickness of approximately 1 nm were successfully synthesized via a simple solvothermal route without any surfactant. Our experiments demonstrated that the ultrathin Rh NSs were formed under the combined effect of both CO and $H_2$, which originate from decomposition of formaldehyde. Such ultrathin Rh NSs presented enhanced the performance of the catalytic oxidation of CO. Ultrathin Rh NSs loaded on $CeO_2$, required lower temperatures for 100% conversion and the starting conversion of CO than Rh nanoparticles. Our proposed route is potentially applicable to synthesizing other noble metal catalysts with an ultrathin structure and a clean surface.

## Acknowledgements

## Notes and references

1 (a) A. R. Tao, S. Habas and P. D. Yang, *Small*, 2008, **4**, 310; (b) L. Zhang, W. X. Niu and G. B. Xu, *Nano Today*, 2012, **7**, 586; (c) Z. Y. Zhou, N. Tian, J. T. Li, I. Broadwell and S. G. Sun, *Chem. Soc. Rev.*, 2011, **40**, 4167.
2 (a) X. Q. Huang, S. H. Tang, X. L. Mu, Y. Dai, G. X. Chen, Z. Y. Zhou, F. X. Ruan, Z. L. Yang and N. F. Zheng, *Nat. Nanotechnol.*, 2010, **6**, 28; (b) Q. Zhang, J. P. Ge, T. Pham, J. Goebl, Y. X. Hu, Z. Lu and Y. D. Yin, *Angew. Chem., Int. Ed.*, 2009, **48**, 3516.

3 (a) M. Chen, B. Wu, J. Yang and N. Zheng, *Adv. Mater.*, 2012, **24**, 862; (b) B. Wu, N. Zheng and G. Fu, *Chem. Commun.*, 2011, **47**, 1039; (c) Y. Dai, X. L. Mu, Y. M. Tan, K. Q. Lin, Z. L. Yang and N. F. Zheng, *J. Am. Chem. Soc.*, 2012, **134**, 7073; (d) X. Q. Huang, S. H. Tang, H. H. Zhang, Z. Y. Zhou and N. F. Zheng, *J. Am. Chem. Soc.*, 2009, **131**, 13916.

4 (a) Y. Yuan, N. Yan and P. J. Dyson, *ACS Catal.*, 2012, **2**, 1057; (b) M. E. Grass, Y. W. Zhang, D. R. Butcher, J. Y. Park, Y. M. Li, H. Bluhm, K. M. Bratlie, T. F. Zhang and G. A. Somorjai, *Angew. Chem., Int. Ed.*, 2008, **47**, 8893.

5 (a) J. D. Hoefelmeyer, K. Niesz, G. A. Somorjai and T. D. Tilley, *Nano Lett.*, 2005, **5**, 435; (b) Y. W. Zhang, M. E. Grass, J. N. Kuhn, F. Tao, S. E. Habas, W. Y. Huang, P. D. Yang and G. A. Somorjai, *J. Am. Chem. Soc.*, 2008, **130**, 5868; (c) S. Kundu, K. Wang and H. Liang, *J. Phys. Chem. C*, 2009, **113**, 18570.

6 (a) N. Zettsu, J. M. McLellan, B. Wiley, Y. D. Yin, Z. Y. Li and Y. N. Xia, *Angew. Chem., Int. Ed.*, 2006, **45**, 1288; (b) Q. A. Yuan, Z. Y. Zhou, J. Zhuang and X. Wang, *Inorg. Chem.*, 2010, **49**, 5515.

7 K. H. Park, K. Jang, H. J. Kim and S. U. Son, *Angew. Chem., Int. Ed.*, 2007, **46**, 1152.

8 K. Jang, H. J. Kim and S. U. Son, *Chem. Mater.*, 2010, **22**, 1273.

9 (a) E. Muller and F. Muller, *Z. Elektrochem. Angew. Phys. Chem.*, 1925, **31**, 41; (b) G. Ertl and J. Tornau, *Z. Phys. Chem.*, 1977, **104**, 301.

10 M. S. Chen, Y. Cai, Z. Yan, K. K. Gath, S. Axnanda and D. W. Goodman, *Surf. Sci.*, 2007, **601**, 5326.

11 (a) A. Trovarelli, *Catal. Rev. Sci. Eng.*, 1996, **38**, 439; (b) J. Zhou, A. P. Baddorf, D. R. Mullins and S. H. Overbury, *J. Phys. Chem. C*, 2008, **112**, 9336.